Performance Monitoring of a Rammed Aggregate Pier Foundation Supporting a Mechanically Stabilized Earth Wall

Mark J. Thompson, Ph.D., M.ASCE[1]; Kord J. Wissmann, Ph.D., P.E.[2]; and Ha T. V. Pham, Ph.D., A.M.ASCE[3]

Abstract: The use of rammed aggregate pier (RAP) foundations for support of retaining walls and earth fill embankments has increased in recent years to become a geotechnical solution for rapid construction of earth structures in soft ground conditions. A nominal 6-m mechanically stabilized earth wall was constructed over piers installed in relatively compressible soil to investigate the performance of RAP foundation elements in terms of stress-deformation and settlement behaviors for such applications. Geotechnical instrumentation consisting of total earth pressure cells, settlement plates, and vibrating wire piezometers was installed within the pier elements and at the foundation surface for short- and long-term monitoring of pier response. Monitoring data indicate: (1) mobilization and concentration of vertical stress on pier elements and matrix soil; and (2) load transfer response for the boundary condition associated with support of geogrid-reinforced earth fill. The practical implications of the experimental research findings are briefly discussed.

DOI: 10.1061/(ASCE)CF.1943-5509.0000010

CE Database subject headings: Retaining walls; Piers; Foundations; Performance characteristics; Load tests; Field tests; Aggregates.

Introduction

The rammed aggregate pier (RAP) system constitutes a ground reinforcement technology that serves as an alternative to deep foundations and overexcavation of compressible soils. This intermediate foundation system was originally used to control excessive settlement of lightly to moderately loaded structures (Lawton and Fox 1994). The RAP system has also increasingly been used to support earth fill embankments and retaining walls (Lien and Fox 2001; Wong et al. 2004), stabilize slopes (Lien and Fox 2001; Kwong et al. 2002; Wissmann et al. 2002; O'Malley et al. 2004; Parra et al. 2007), and mitigate seismic hazards (Girsang et al. 2004). With a growing number of successful case histories involving RAPs in difficult ground conditions for various transportation applications, researchers have continued to investigate the behavior and support mechanisms of the foundation elements.

This paper describes a field experiment in which the performance of RAPs supporting a mechanically stabilized earth (MSE) wall was monitored. The main objectives of the study are to: (1) document the performance of RAPs for support of the MSE wall; and (2) describe the stress-deformation behavior of RAPs in connection with governing load transfer mechanisms. As a limited number of detailed studies concerning the performance of RAPs for support of geogrid-reinforced earth fill have been documented, findings from the experimental research study described herein may be useful to both researchers and practitioners.

Site Investigation

The subsurface profile at the project site consists of soft, nonuniform loessial clay classifying as sandy lean clay (CL) to a depth of approximately 4 to 5 m. This soil layer is underlain by comparatively stiffer, locally discontinuous glacial till. Groundwater was encountered approximately 1 m below the ground surface. Engineering and index properties of the soft clay were evaluated using both laboratory and in-situ testing methods. The test results are summarized in Table 1. Natural moisture content ranged from 17.4 to 41.2%. Liquid limit and plastic index values were 40 and 20%, respectively. Undrained shear strength based on unconfined compression tests ranged from 12.2 to 59.0 kPa. A consolidated-undrained triaxial test showed an effective stress friction angle (ϕ') of 28° and cohesion (c') of 2.4 kPa. Based on the in-situ borehole shear tests, the internal friction angle of the soil ranged from 16.7 to 35.0° and cohesion ranged from 0.0 to 18.5 kPa. Six one-dimensional consolidation tests were performed with values of compression index ranging from 0.16 to 0.37.

Cone penetration tests (CPT) were performed at two locations within the wall footprint (e.g., Center and North) for defining the soil profile and identifying soil behavior. CPT data are shown in Fig. 1. Tip resistance of the soil within the pier length ranged from 1 to 7 MPa, while friction ratios generally ranged up to about 8 percent. Only the CPT profile at the north end of the wall footprint area identified the glacial till material at a depth of 4–5 m, though drilling behavior and soil samples provided evidence of this soil layer existing at other locations beneath the wall. Following the installation of RAPs, cone penetration testing was repeated at the center of the full-height wall section to demonstrate the effect of pier installation on soil behavior. CPT data

[1]Staff Geotechnical Engineer, CH2M HILL, 1100 112th Avenue, Suite 400, Bellevue, WA 98004. E-mail: mark.thompson@ch2m.com

[2]President and Chief Engineer, Geopier Foundation Company, 150 Fairview Road, Mooresville, NC 28117. E-mail: kwissmann@geopier.com

[3]Staff Geotechnical Engineer, CH2M HILL, 1100 112th Avenue, Suite 400, Bellevue, WA 98004. E-mail: ha.pham@ch2m.com

Note. This manuscript was submitted on May 16, 2008; approved on December 11, 2008; published online on July 15, 2009. Discussion period open until January 1, 2010; separate discussions must be submitted for individual papers. This paper is part of the *Journal of Performance of Constructed Facilities*, Vol. 23, No. 4, August 1, 2009. ©ASCE, ISSN 0887-3828/2009/4-244–250/$25.00.

Table 1. Laboratory and In Situ Test Results

Depth (m)	γ_d (kN/m^3)	w (%)	S_u (kPa)	C_c[a]	C_s[b]	C_{ec}[a]	C_{es}[b]	ϕ' (degrees)	c' (kPa)
0.25	13.69	41.2	41.8	—	—	—	—	—	—
0.33[d]	—	—	—	—	—	—	—	35.0	0.0
0.36[d]	—	—	—	—	—	—	—	25.4	18.5
0.36	11.51	38.9	—	0.37	0.04	0.160	0.016	—	—
0.51	15.23	22.7	—	0.20	0.03	0.113	0.019	—	—
0.94	15.64	27.5	12.2	—	—	—	—	—	—
1.07	14.70	24.8	—	0.20	0.03	0.103	0.017	—	—
1.07[d]	—	—	—	—	—	—	—	24.2	11.0
1.14[c]	17.50	20.2	—	—	—	—	—	28.0	2.4
1.17[d]	—	—	—	—	—	—	—	16.7	18.0
1.22	17.27	24.0	59.0	—	—	—	—	—	—
1.28[c]	18.17	17.4	—	—	—	—	—	28.0	2.4
1.57	15.54	22.0	—	0.18	0.03	0.096	0.019	—	—
1.78	17.75	20.8	39.1	—	—	—	—	—	—
1.83	16.55	20.8	—	0.16	0.03	0.085	0.018	—	—
2.01[c]	17.09	27.4	—	—	—	—	—	28.0	2.4
2.64	18.03	22.0	59.2	—	—	—	—	—	—
2.74	15.52	22.0	—	0.20	0.03	0.112	0.018	—	—

[a]Compression index from one-dimensional consolidation test.

[b]Calculated from unload curve in one-dimensional consolidation test.

[c]Consolidated-undrained triaxial test.

[d]In situ borehole shear test. 1 kN/m^3=6.37 lb/ft^3, 1 kPa=20.9 lb/ft^2.

for this test are also provided in Fig. 1. Results obtained from the CPT performed after pier installation showed a slight increase in tip resistance and a significant reduction in sleeve friction. Reduced sleeve friction may indicate plastic remolding of soil adjacent to the RAPs and loss of soil cohesion, as also suggested by Handy and White (2006).

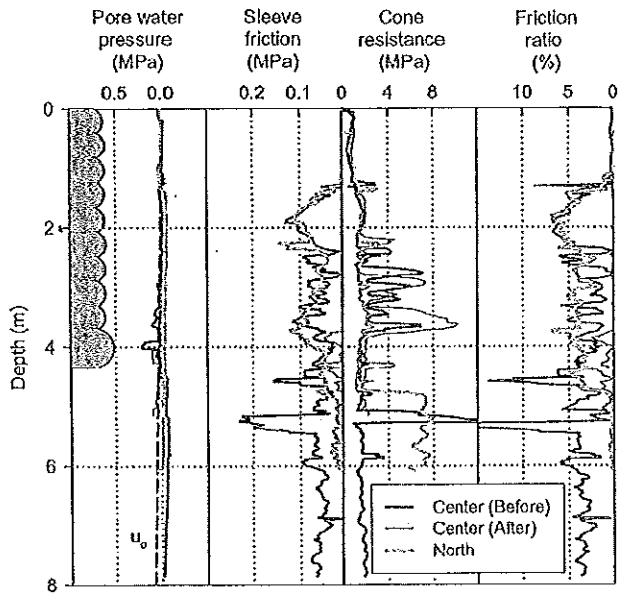

Fig. 1. CPT results for foundation soils at center of full-height wall section before and after pier installation and at north end of wall footprint area before pier installation

Design and Construction

The MSE wall was designed by Tensar Earth Technologies, Inc. as a flexible faced wall system. Design details of the wall and supporting pier elements are provided in Fig. 2. The construction sequence is illustrated in Figs. 3(a–f). Plan dimensions of the nominal 6-m wall are 4.5 m×4.5 m. The (2:1) sideslopes yield a base width of about 28 m. Granular backfill was reinforced using nine layers of UX-1100 uniaxial reinforcement and three layers of BX-1100 biaxial reinforcement with lengths of 3.6 and 1.2 m, respectively. The L-shaped welded-wire facing units were 0.46 m×0.46 m. Diagonal support struts provided lateral resistance to compaction-induced stresses and also served as connectors for the geogrid reinforcement. A geotextile filter placed inside of the facing units retained the granular backfill material.

The granular backfill classified as poorly graded sand (C_u =2.75, C_c=1.11, D_{10}=0.2 mm). The material for each 0.46 m layer was placed in two lifts and compacted using vibratory plate compactors. Compaction energy associated with two or three passes was applied to the material. The moisture content and total unit weight of the compacted material was measured using a nuclear moisture-density gauge. Based on 110 tests performed in different wall layers, the mean total unit weight was 16.57 kN/m^3 with a standard deviation of 0.57 kN/m^3. The average vertical overburden pressure at the foundation surface after construction of the 5.94-m wall was about 98 kPa.

The MSE wall was supported by 22 RAPs with lengths ranging from 3.8 to 4.6 m. The piers were installed in four rows with center-to-center spacing of 1.5 m. The area replacement ratio (R_a), defined as the ratio of pier cross-sectional area to total area, was about 0.20. The pier lengths were selected with the intention of having pier tips rest on the glacial till layer located about 4–5 m below the ground surface. Pier installation, as

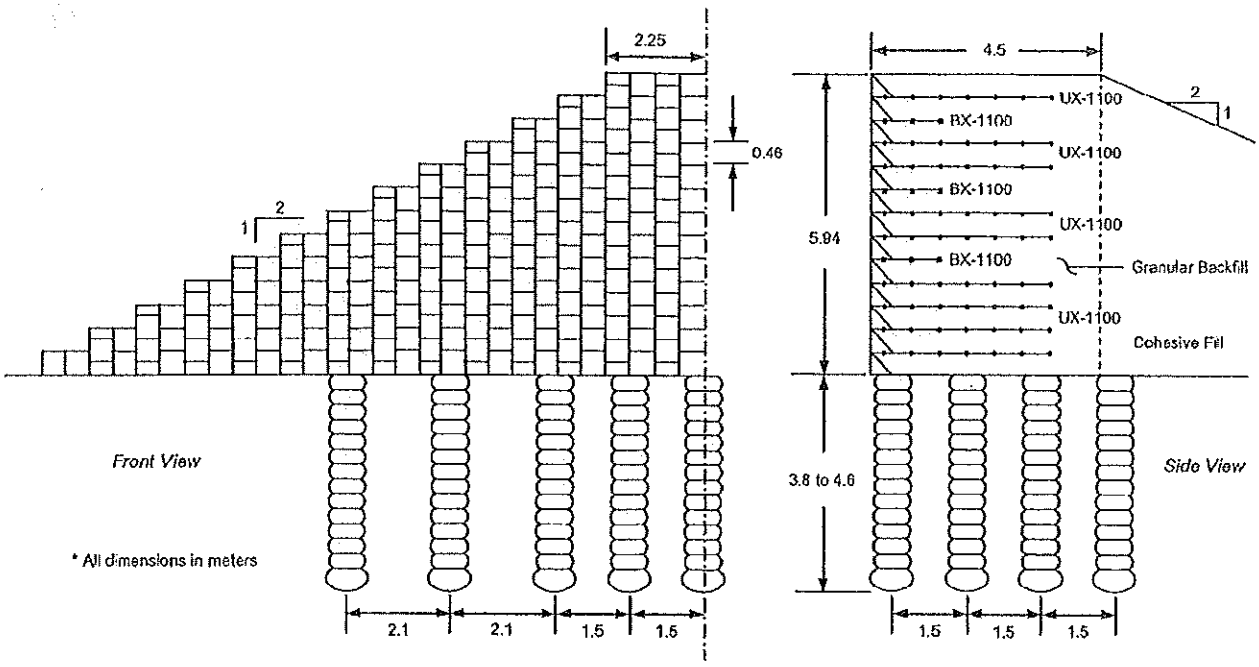

Fig. 2. Design of MSE wall and rammed aggregate pier support

shown in Fig. 3(a), began with the drilling of a 0.76-m diameter cavity. Crushed stone classifying as poorly-graded gravel (C_u = 1.8, C_c=0.7, D_{10}=18 mm) was then placed in layers with nominal thickness of 0.3 m and compacted using a beveled tamper connected to a hydraulic rammer. The result of the pier construction process was a column of densely-compacted aggregate surrounded by comparatively weaker matrix soil. Details of the pier construction process can be found in Lawton and Fox (1994), Wissmann and Fox (2000), and Handy and White (2006).

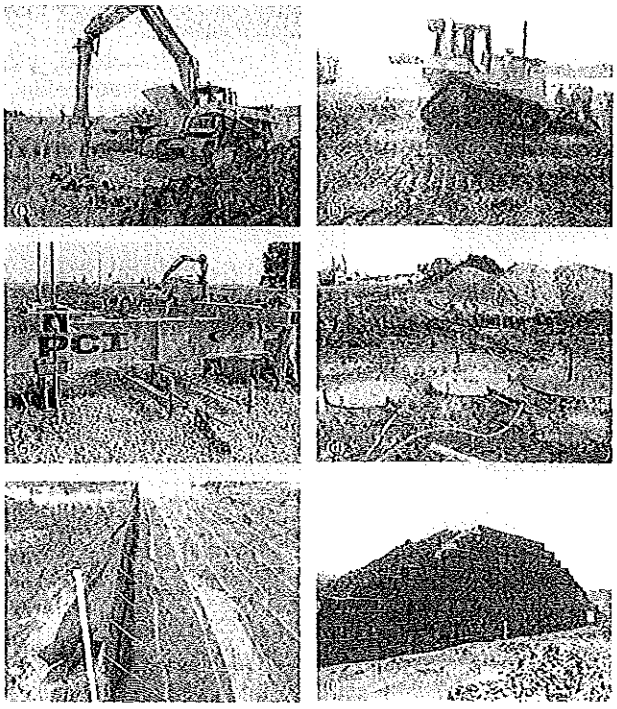

Fig. 3. Construction sequence: (a) pier installation; (b) site grading; (c) modulus load test; (d) instrumentation installation; (e) MSE wall components; and (f) completed MSE wall

Instrumentation

The instrumentation plan was developed primarily to monitor vertical stress and settlement of pier elements and matrix soil. The instrumentation is summarized in Fig. 4. Four 0.23 m total earth pressure cells (EPC) were installed within Piers 11 and 12 at depths of 0.91, 2.13, and 3.05 m during pier installation. Six EPCs (0.23 and 0.71 m) were also placed on the foundation surface [see Fig. 3(d)] to measure vertical stress increases on top of the piers (EPC-1, EPC-3, EPC-5) and the matrix soil (EPC-2, EPC-4, EPC-6). Four circular, steel settlement plates (SP) with diameters of 0.76 m were installed on the foundation surface to measure pier and matrix soil settlement. Of the settlement plates placed on matrix soil, SP-2 was located in the pier-reinforced zone, whereas SP-3 was located in the unreinforced zone behind the last row of piers. Two vibrating wire piezometers (PZ) were installed immediately behind Pier 5 at depths of 2.0 and 3.8 m. Piezometer measurements were used predominantly to monitor the variation of excess pore pressures during and after pier installation, as well as during consolidation of foundation soils. For brevity, the pore pressure data are not reported in this paper.

Stress-Deformation Response

The deformation behavior of an isolated RAP was evaluated by conducting a full-scale modulus load test at the wall site [see Fig. 3(c)]. The load test was conducted on a sacrificial pier 4.3 m in length with telltales placed 3.6 m below the ground surface.

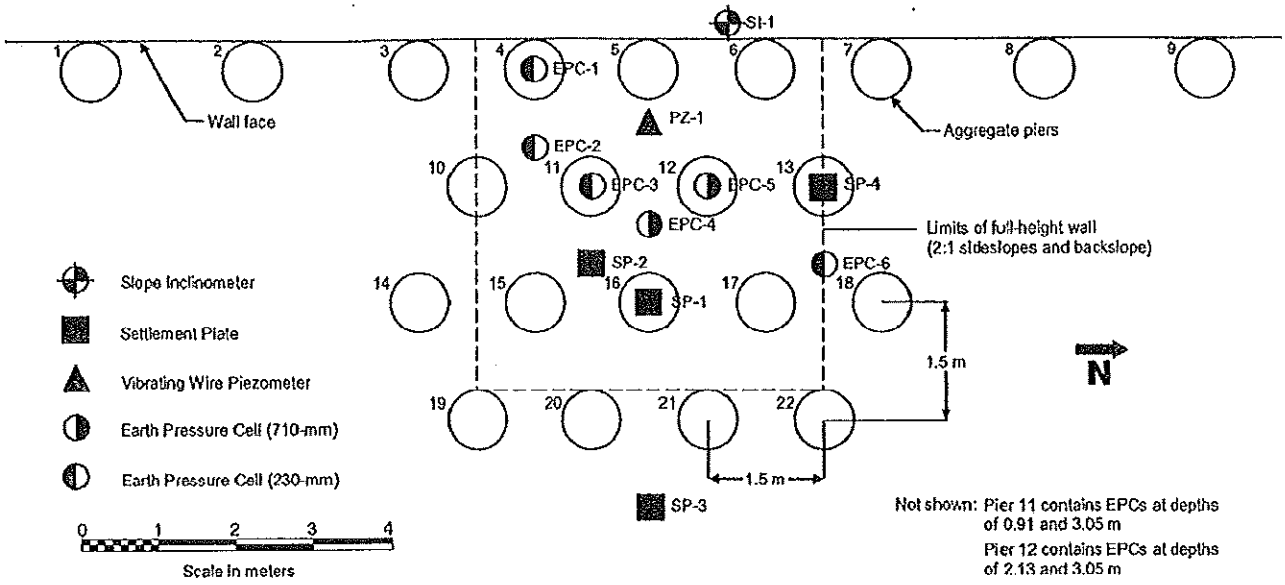

Fig. 4. Pier layout and foundation instrumentation plan

The stress-controlled test was performed by applying nominal load increments of 75 kN to the concrete cap and measuring pier settlement using dial gauges. The stress-deformation response of the tested pier is provided in Fig. 5. The increasing difference in settlement of the pier cap and telltales observed with increasing pier stress is interpreted as pier bulging. This mode of deformation has been noted to be prevalent for pier lengths exceeding about three diameters (White and Suleiman 2005), particularly when the pier tip rests on a bearing soil layer. Stress-dependent stiffness behavior was determined by calculating pier stiffness as the ratio of applied compressive stress to pier settlement at each stage of the modulus load test. This stiffness response is provided in Fig. 6 as a function of pier settlement.

Performance Monitoring Results

Stress Concentration

The vertical contact stresses measured on top of piers and matrix soil at five stages of MSE wall construction are provided in Fig. 7. The overburden stresses recorded by all pressures cells placed on matrix soil were similar to each other at all stages of construction. The vertical stress measured by EPC-1 was considerably higher than those recorded by other pressure cells placed on piers, likely because this pressure cell was placed on a perimeter pier where a portion of the surcharge load could not be carried by an adjacent pier through soil arching. Shortly after construction, the stress concentrated on top of the pier elements averaged about 253 kPa, while the average stress distributed to the matrix soil was about 59 kPa. Stress measurements of EPC-1 decayed from about 310 kPa to about 240 kPa in the 25 days following fill placement, which reduced the long-term average pier stress to a value of approximately 230 kPa. Because Dunnicliff (1993) indicates that the measurement of pressure mobilized on soft soil can be inaccurate, the accuracy of instrumentation data was evaluated by multiplying the pier stress by R_a and by multiplying the matrix soil stress by $(1\text{-}R_a)$. The sum of these products is a weighted average equaling about 95 kPa. The agreement between this weighted average and the calculated overburden pressure based on backfill density measurements (98 kPa) supports the monitoring results of total earth pressure cells.

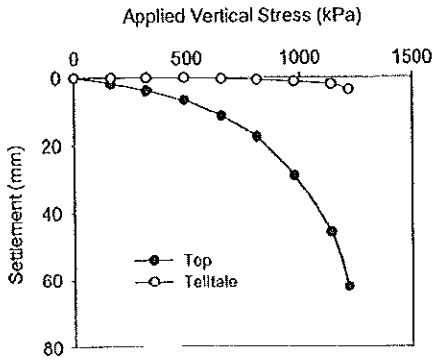

Fig. 5. Stress-deformation behavior of isolated aggregate pier from modulus load test

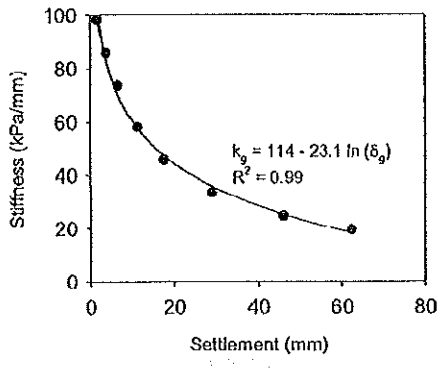

Fig. 6. Stress-dependent stiffness behavior of isolated rammed aggregate pier from modulus load test

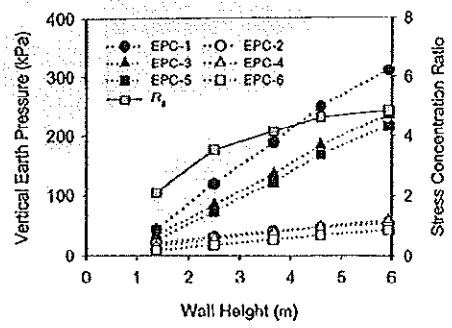

Fig. 7. Vertical earth pressure measurements and stress concentration ratio calculated from average vertical stresses

Fig. 7 shows the stress concentration ratio (R_s) at the foundation surface, which is calculated as the ratio of top-of-pier stress to matrix soil stress. R_s increases from about 2.1 to 4.9 as the wall height increases from 1.4 to 5.9 m. The increase in stress concentration ratio likely results from nonlinear soil behavior and nearly elastic pier behavior in the range of working foundation stress. The increased matrix soil settlement (relative to the piers) observed with higher surcharge loads promotes soil arching and stress concentration on the piers. Using the stress concentrated on matrix soil at the foundation surface and the vertical pier stress approximately 1.2 d_{pier} below the foundation grade (520 kPa), a stress concentration value of about 8.8 is calculated; the higher stress concentration observed below the foundation surface is attributed to the load transfer along the pier length, which is described in a later section. Stress concentration ratios produced by the performance monitoring results of this study agree reasonably well with values ranging from 1 to 11 for RAPs in soft ML and CL soils, as documented in Warner (2003), Lawton and Warner (2004), and White et al. (2007).

Settlement and Stiffness Responses

The long-term settlement response of the foundation is provided in Fig. 8. Pier settlement measurements for SP-1 and SP-4 were identical, such that pier settlement is presented using only one symbol. The sudden increases in settlement resulted from fill placement, which occurred on days 1, 2, 4, 5, and 12. Measurements show that the piers, matrix soil, and unreinforced soil had settled about 22, 30, and 133 mm, respectively, immediately following completion of fill placement. Interbedded sand layers within the upper 5 m of the foundation soil (see Fig. 1) and possibly the aggregate pier itself expedited consolidation of the highly compressible layer. This interpretation of foundation

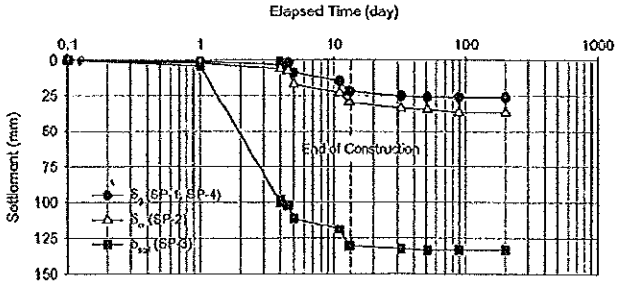

Fig. 8. Foundation settlement results

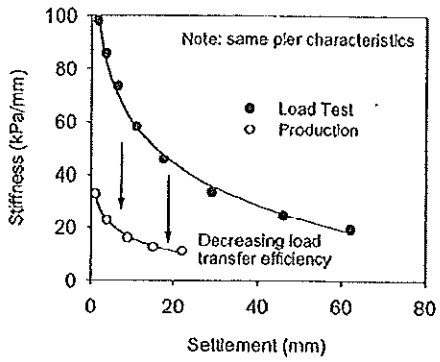

Fig. 9. Comparison of calculated stiffness based on top-of-pier stress for isolated pier from modulus load test and production piers supporting the MSE wall indicating reduced load transfer efficiency

settlement response was supported by rapid dissipation of excess pore pressures measured using the vibrating wire piezometers. The ratio of top-of-pier settlement to reinforced matrix soil settlement is 0.73. The unreinforced foundation soil settled about 4.4 times more than reinforced soil.

Fig. 9 provides the stiffness of production piers, calculated using top-of-pier stress and settlement data. The stiffness values obtained from the modulus load test are also provided in Fig. 9 for comparison. The stiffness response of production piers supporting the MSE wall (based on top-of-pier stress measurements) appears to be considerably lower than that obtained from the modulus load test on the test pier. This apparent difference in the stiffness response between the test and production piers does not reflect a difference in pier characteristics or behavior, but rather a difference in boundary condition resulting from comparatively inefficient load transfer to piers for the case of production piers supporting the MSE wall. The observed load transfer behavior of RAPs supporting geogrid-reinforced earth fill is described in the following sections.

Load Transfer

Total earth pressure cells were used to monitor the vertical stress distribution in Piers 11 and 12 during pier installation and MSE wall construction. The profile of vertical stress increase (within the pier) resulting from fill placement is provided in Fig. 10. The stress increase was calculated as the difference between the total

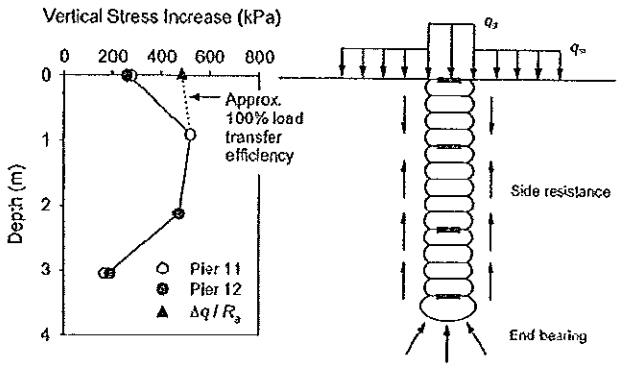

Fig. 10. Vertical stress increase within rammed aggregate piers and interpretation of load transfer

vertical stress measured at the end of construction and the initial vertical stress after pier construction. The vertical pier stress is shown to increase from about 253 kPa at the pier top to about 520 kPa at 0.91 m ($1.2\ d_{pier}$) below the foundation surface. Below 0.91 m, the vertical stress decreases nonlinearly to about 181 kPa at 3.05 m ($4.0\ d_{pier}$). Also provided in Fig. 10 is an estimate of the maximum vertical pier stress assuming complete soil arching. By applying the overburden weight only to the pier cross-sectional area, the theoretical maximum stress is calculated as the ratio of the overburden pressure to the area replacement ratio. The estimate of maximum vertical pier stress is 483 kPa, about 7 percent less than measured with total earth pressure cells at a depth of 0.91 m. The apparent difference between the theoretical maximum and that measured with instrumentation might be attributed to either: (1) stress concentration on the pressure cell within the pier element as a result of the difference in stiffness of the plate and the pier material; or (2) slight variation in the stiffness of production piers that causes more load to be concentrated on the stiffer piers of the group. The stiffness of different production piers may vary as a result of variable compaction energy delivered to the pier during construction or variable soil conditions affecting pier installation (i.e., stiffer matrix soil generally produces stiffer pier elements). In this case of variable pier stiffness, more load is likely to concentrate on the stiffer piers than adjacent piers with lower stiffness. The variation of vertical pier stress at the foundation surface can be seen in Fig. 7.

The load transfer shown in Fig. 10 results from the surcharge loads being applied through a nonrigid platform with the consequence being that the settlement of matrix soil around the piers exceeds the settlement of piers (see Fig. 8)—an occurrence not seen with pier support of rigid footings. The load on the matrix soil is transmitted to the comparatively stiffer pier elements through shear at the pier-soil interface in the upper potion of the pier. This behavior is analogous to negative skin friction or "downdrag" of deep foundations. Data in Fig. 10 show vertical stress mobilization of 520 kPa at a depth 0.91 m, which is about twice as large as the vertical stress increase at the pier top. Because this load transfer mechanism increases the vertical pier stress below the foundation elevation, pier stiffness calculated using the top-of-pier stress is reduced (see Fig. 9).

Behavior of RAP Groups Supporting Geogrid-Reinforced Earth Fill

The difference in stiffness between matrix soil and piers supporting MSE walls or embankments results in stress concentration on the piers. This stress concentration, which gives pier stress considerably higher than vertical overburden pressure, is mobilized through differential settlement between the piers and matrix soil and development of a soil arch in the overburden material. Alternatively, the stress concentration observed in a pier group supporting a rigid footing is principally attributed to the difference in stiffness of the piers and matrix soil, where the footing imposes strain compatibility between the elements.

The stiffness of an isolated pier based on a modulus load test has been shown by White et al. (2007) to represent a practical approach for the design and analysis of pier groups supporting rigid footings. However, the current study suggests that the different loading conditions and load transfer mechanisms of pier groups for cases of support of footings and geogrid-reinforced earth fill must be considered during design. The vertical stress concentrated on the top of piers supporting earth fill is less than for piers supporting a rigid footing. This response results from comparatively inefficient load transfer to the pier elements at the foundation (top-of-pier) elevation, which is also supported by differential settlements measured between the piers and matrix soil. Because earth fill does not impose a rigid boundary condition, the stress which is applied to matrix soil at the foundation surface is transferred to the adjacent piers through shear along the pier-soil interface. This load transfer response is supported by data in Fig. 10 showing increasing vertical pier stress with depth below the foundation surface. The below-grade load transfer behavior moves the effective top-of-pier elevation deeper, where the below-grade vertical pier stress approximately corresponds to total surcharge load transfer. The practical implication of this response is a reduced effective pier length for transferring pier stresses to foundation soils. The load transfer efficiency for RAPs supporting a mechanically stabilized earth wall or earth fill embankment may be increased by constructing a stiffer load application device, such as a platform comprised of stiff, closely-spaced geogrid immediately overlying the RAP foundation.

Summary and Conclusions

The RAP foundation for a nominal 6-m MSE wall was instrumented with total earth pressure cells and settlement plates for long-term performance monitoring and investigation of the behavior of RAPs for support of geogrid-reinforced earth fill. The data collected during construction of the MSE wall and following fill placement indicate the following:

1. Stress concentration ratios at the top of the piers ranged from 2.1 to 4.9 and increased with overburden pressure. These values are generally less than for pier groups supporting rigid footings. Stress concentration for support of geogrid reinforced earth fill should also depend on tensile stiffness and arrangement of the reinforcement.
2. Using the stress concentrated on matrix soil at the foundation surface and the vertical pier stress approximately $1.2\ d_{pier}$ below the foundation grade, a stress concentration value of about 8.8 is calculated. The higher stress concentration observed below the foundation surface is attributed to the load transfer along the pier length.
3. RAPs provide significant settlement mitigation potential, with settlement reduced from 130 mm for unreinforced soil to about 22 mm for RAPs (six-fold reduction).
4. The vertical stress distribution observed within pier elements indicates significant load transfer from the matrix soil to the pier elements in the upper potion of the pier. The below-grade load transfer behavior moves the effective top-of-pier elevation deeper, thereby decreasing the effective pier length for transferring pier stresses to foundation soils.

Acknowledgments

This research was sponsored by Geopier Foundation Company, Inc. and Iowa State University. This material is also based upon work supported under a National Science Foundation Graduate Research Fellowship. The writers are grateful for this sponsorship. The MSE wall was designed by Tensar Earth Technologies, Inc. Brendan FitzPatrick, Associate Project Engineer with Geopier Foundation Company, designed the RAP foundation. Peterson Contractors, Inc. of Reinbeck, Iowa installed the RAPs and constructed the MSE wall. The writers would also like to

acknowledge David White, Associate Professor at Iowa State University, for his oversight of the research program and Thang Phan, graduate student at Iowa State University, for assisting with the site investigation and instrumentation installation.

Notation

The following symbols are used in this paper:

C_c = compression index;
C_s = swell index;
C_u = coefficient of uniformity;
c' = effective cohesion;
D_{10} = 10th percentile particle size;
d_{pier} = pier diameter;
e_0 = initial void ratio;
H_c = thickness of compressible soil layer;
k_g = stiffness of pier element;
k_m = stiffness of matrix soil;
q = vertical overburden pressure;
q_g = stress concentrated on pier element;
q_m = stress concentrated on matrix soil;
q_0 = initial vertical stress at mid-layer depth;
R_a = area replacement ratio;
R_s = stress concentration ratio;
s_u = undrained shear strength;
w = moisture content;
γ_d = dry unit weight;
δ = settlement;
δ_g = settlement of pier element;
δ_m = settlement of matrix soil;
δ_{soil} = settlement of unreinforced soil;
Δq = vertical stress increase at midlayer depth; and
ϕ' = effective internal friction angle.

References

Dunnicliff, J. (1993). *Geotechnical instrumentation for monitoring field performance*, Wiley, New York.

Girsang, C., Gutierrez, M., and Wissmann, K. (2004). "Modeling of the seismic response of the aggregate pier foundation system." *Proc., GeoSupport 2004*, ASCE, GSP No. 124.

Handy, R., and White, D. (2006). "Stress zones near displacement piers. I: Plastic and liquefied behavior." *J. Geotech. Geoenviron. Eng.*, 132(1), 54–62.

Kwong, H., Lien, B., and Fox, N. (2002). "Stabilizing landslides using rammed aggregate piers." *Proc., 5th Malaysian Road Conf.*, Kuala Lumpur, Malaysia.

Lawton, E., and Fox, N. (1994). "Settlement of structures supported on marginal or inadequate soils stiffened with short aggregate piers." *Proc., Vertical and Horizontal Deformations of Foundations and Embankments*, ASCE, Reston, Va.

Lawton, E. C., and Warner, B. J. (2004). "Performance of a group of geopier elements loaded in compression compared to single geopier elements and unreinforced soil." *Rep. No. UUCVEEN 04-12*, Univ. of Utah.

Lien, B., and Fox, N. (2001). "Case histories of geopier soil reinforcement for transportation applications." *Proc., Asian Institute of Technology Conf.*, Bangkok.

O'Malley, E., Saunders, S., and Ecker, J. (2004). "Slope rehabilitation at the Baltimore-Washington Parkway using rammed aggregate piers." *Proc., TRB 2004 Annual Meeting* (CD-ROM), Washington, D.C.

Parra, J., Caskey, M., Marx, E., and Dennis, N. (2007). "Stabilization of failing slopes using rammed aggregate pier reinforcing elements." *Proc., Geo-Denver 2007: Soil Improvement* (CD-ROM), GSP No. 172, Denver.

Warner, B. J. (2003). "Settlement and bearing capacity improvement with pier groups." Master's thesis submitted to Dept. of Civil and Environmental Engineering, Univ. of Utah.

White, D., Pham, H., and Hoevelkamp, K. (2007). "Support mechanisms of rammed aggregate piers. I: Experimental results." *J. Geotech. Geoenviron. Eng.*, 133(12), 1503–1511.

White, D., and Suleiman, M. (2005). "Design of short aggregate piers to support highway embankments." *Transportation Research Record. 1868*, National Academy, 103–112.

Wissmann, K., FitzPatrick, B., White, D., and Lien, B. (2002). "Improving global stability and controlling settlement with geopier soil reinforcing elements." *Proc., 4th Int. Conf. on Ground Improvement Techniques*, Kuala Lumpur, Malaysia.

Wissmann, K., and Fox, N. (2000). "Design and analysis of short aggregate piers used to reinforce soil for foundation support." *Proc., Darmstadt Technical University Colloquium*, Darmstadt, Germany.

Wong, D., FitzPatrick, B., and Wissmann, K. (2004). "Stabilization of retaining walls and embankments using rammed aggregate piers." *Proc., Geo-Trans 2004: Geotechnical Engineering for Transportation Projects*, GSP No. 126, Vol. 2.